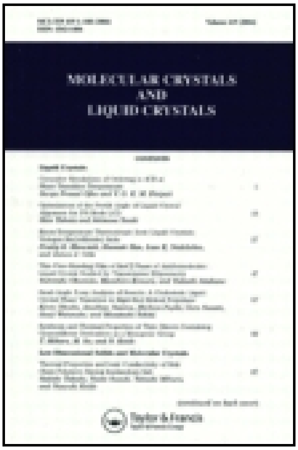

Molecular Crystals and Liquid Crystals Science and Technology. Section A. Molecular Crystals and Liquid Crystals

Publication details, including instructions for authors and subscription information:
http://www.tandfonline.com/loi/gmcl19

Structural Studies of Cetyltrimethylammonium Chloride and its Complex with p-Phenylphenol

Kenji Okuyama [a] , Tomie Ishii [a] , Kulthida Vongbupnimit [a] & Keiichi Noguchi [a]

[a] Faculty of Technology, Tokyo University of Agriculture and Technology, Koganei, Tokyo, 184, Japan

Version of record first published: 04 Oct 2006

To cite this article: Kenji Okuyama, Tomie Ishii, Kulthida Vongbupnimit & Keiichi Noguchi (1998): Structural Studies of Cetyltrimethylammonium Chloride and its Complex with p-Phenylphenol, Molecular Crystals and Liquid Crystals Science and Technology. Section A. Molecular Crystals and Liquid Crystals, 312:1, 101-115

To link to this article: http://dx.doi.org/10.1080/10587259808042434

Mol. Cryst. Liq. Cryst., 1998, Vol. 312, pp. 101–115
Reprints available directly from the publisher
Photocopying permitted by license only

Structural Studies of Cetyltrimethylammonium Chloride and its Complex with *p*-Phenylphenol

KENJI OKUYAMA*, TOMIE ISHII, KULTHIDA VONGBUPNIMIT
and KEIICHI NOGUCHI

*Faculty of Technology, Tokyo University of Agriculture and Technology,
Koganei, Tokyo 184, Japan*

(Received 1 August 1997; In final form 25 September 1997)

According to the temperature-composition phase diagram of cetyltrimethylammonium chloride (CTAC) and *p*-phenylphenol (*p*-PP), which was obtained by DTA measurement of powder mixtures at various composition ratios, it was found that only one complex with a 1/1 molar ratio was available for the CTAC/*p*-PP system. The single crystal structure of this complex, together with the crystal structure of CTAC, was determined by the X-ray diffraction method. Both crystals have a smectic layer structure stacked along the *c*-axis. The CTAC (and *p*-PP) molecules are arranged almost perpendicular to the layer surface. Within the smectic layer of the host (CTAC) crystal, long alkyl chains from both sides of layer surfaces are interdigitated mutually, which makes a hydrophobic region in the middle of the layer. In complex (CTAC/*p*-PP) crystals, guest (*p*-PP) molecules were accommodated in the space formed by loosening their interdigitation. The arrangement of *p*-PP molecules found in the complex crystal is very similar to that in the *p*-PP crystal. The thermal behavior of complex crystals is also very similar to that of *p*-PP. Therefore, the complex structure seemed to be highly influenced by the guest–guest interaction. We call this type of complex structure a "guest-dependent" structure.

Keywords: Complex formation; amphiphilic molecules; crystal structures; cetyltrimethylammonium chloride

---

*Corresponding author. Tel.: -81-423-88-7028. Fax: -81-423-88-7209. e-mail: okuyamak@cc.tuat.ac.jp.

INTRODUCTION

Amphiphilic molecules with long hydrophobic alkyl chains, such as phospholipids in biological membranes and synthetic surfactants, can aggregate spontaneously in an aqueous solution. These aggregations can take various types of higher order organization, such as a bimolecular layer arrangement, spherical micelles and rod-shaped micelles. Here, the structural differences between these organizations depend mainly on their chemical structures and concentrations. In the solid state, however, most of amphiphilic molecules take very similar two-dimensional smectic layers. These layers stack along the normal direction to the layer surface to make a three-dimensional crystal structure. The molecular arrangement in the smectic layer depends on the chemical structure of an element amphiphile. For example, in the cases of dialkyldimethylammonium salts, amphiphiles can form a bimolecular layer with some tilt to compensate for the difference of cross-sections between the hydrophilic head part and the hydrophobic tail part [1, 2]. On the other hand, in the cases of monoalkyltrimethylammonium salts, [3] alkyl long chains from both sides of the layer surfaces are packed together in an interdigitating manner to compensate for the large hydrophilic head part. Therefore, the thickness of the smectic layer is usually similar to the molecular length of this amphiphile, while the thickness of a smectic layer composed of dialkyldimethylammonium slats is usually larger than the molecular length but smaller than the bimolecular length.

Recently, it was found that monoalkyltrimethylammonium salts can be crystallized with various aromatic compounds to form crystalline clathrate compounds [4–8]. Interestingly, the formation of clathrate compounds is available not only by recrystallization from their solution, but also by mixing host and guest crystalline powders in a mortar [7, 8]. To get a better understanding of host-guest interactions in these clathrate compounds, we are studying various clathrates and host compounds from the structural point of view. In this manuscript, cetyltrimethylammonium chloride (CTAC, host) and its clathrate CTAC/*p*-phenylphenol (*p*-PP, guest) complex structures have been analysed.

EXPERIMENTAL

Samples of cetyltrimethylammonium chloride (CTAC), *p*-phenylphenol (*p*-PP) and 1-naphthol were purchased from Tokyo Chemical Industry Co., Ltd.

Construction of Phase Diagram for CTAC/*p*-PP System

Mixed powder samples of CTAC and *p*-PP at various molar ratios were prepared by grinding for about 40 minutes in a mortar until powders became uniform. Thermal behaviors of these samples were observed by thermogravimetric analysis and differential thermal analysis (TG-DTA 8110) on a Rigaku TAS-100 system at a heating rate of 10°C/min with nitrogen purge gas at a flow rate of 35 ml/min. Each phase was investigated by an optical microscopic observation (SZH-10, Olympus) and a powder X-ray diffraction method (DIP-100, MAC Science Co., Ltd. and RAD-C, Rigaku). X-ray diffraction patterns from samples in a home-made heating cell were recorded on an imaging plate (DIP-100) at various temperatures, while X-ray diffraction curves were recorded on a chart (RAD-C) at room temperature.

Single Crystal Preparation and Data Collection

Colorless, prismatic single crystals of CTAC were grown from the mixed solution of ethylacetate and acetone in which CTAC and 1-naphthol were dissolved at a 1/1 molar ratio. In spite of our trial to get single crystals of the CTAC/1-naphthol complex, we obtained only single crystals of CTAC hydrate. On the other hand, all the trials to get single crystals of monoalkyltrimethylammonium chlorides including CTAC have been unsuccessful. The compound, 1-naphthol, may play some part in crystallization of CTAC. Colorless, platelike, single crystals of the CTAC/*p*-PP complex were obtained by keeping the ethylacetate solution of CTAC and *p*-PP at 1/1 molar ratio in the incubator at 20°C. Both crystals took about 1 week to grow to suitable size for X-ray diffraction study.

A crystal of CTAC (0.20 × 0.20 × 0.30 mm) and a crystal of CTAC/*p*-PP complex (0.15 × 0.10 × 0.20 mm) were used for the intensity measurement by a Rigaku AFC7R and AFC5R diffractometer, respectively. A graphite monochromated CuKα radiation (λ = 1.5418 Å) from a Rigaku rotating anode X-ray generator was used for both measurements. Cell constants and an orientation matrix for data collection were obtained from a least-squares refinement using the setting angles of 24 carefully centered reflections in the range of $78.06 < 2\theta < 80.00°$ for CTAC and 25 reflections in the range of $27.71 < 2\theta < 45.42°$ for the CTAC/*p*-PP complex. Parameters for data collection and crystal data are listed in Table I. Since intensities of standard reflections of CTAC decreased by 18.6% during the data collection, a polynomial correction factor was applied, while no decay was observed for

TABLE I Parameters for data collection and cyrstal data

Compound	*CTAC*	*CTAC/p-PP*
Formula	$C_{19}H_{42}NCl{\cdot}O.5H_2O$	$C_{19}H_{42}NCl \cdot C_{12}H_{10}O$
Molecular weight	329.01	490.21
Space group	$P\bar{1}$	$P2_1/a$
a/Å	19.499(3)	9.921(2)
b/Å	8.6228(9)	10.121(1)
c/Å	27.091(6)	31.970(4)
α/°	92.47(2)	90.00
β/°	77.00(2)	92.14(1)
γ/°	78.44(2)	90.00
V/Å^3	4329(4)	3207.9(8)
Z	8	4
μ(CuKα)/cm^{-1}	15.6	11.9
Dobs/g cm^{-3}	–	1.02
Dcal/g cm^{-3}	1.03	1.015
F(0 0 0)	1504.0	1080.0
Scan mode	$\omega-2\theta$	$\omega-2\theta$
Scan speed/° (in ω) min^{-1}	16	16
Scan width/° (in ω)	$1.84+0.30\tan\theta$	$2.00+0.30\tan\theta$
Maximum 2θ/°	120	120
No. of observed reflections	Total: 13305 Unique: 12865	Total: 5425 Unique: 5091
No. of reflections used for refinement	6250 $Io > 3\sigma(Io)$	1267 $Fo > 4\sigma(Fo)$

CTAC/*p*-PP. Both intensity data were corrected for Lorentz and polarization effects. Absorption corrections based on azimuthal scans were also carried out.

Structure Determination and Refinement

Both structures were solved by the direct method using the program SHELX-86 [9] and expanded by using Fourier techniques. The non hydrogen atoms were refined anisotropically. Hydrogen atoms were introduced by geometrical calculations but not refined. The final cycles of full-matrix least-squares refinement for CTAC were based on 6,250 reflections and 776 variable parameters. In these calculations, the 001 reflection was removed from the data set because of the disagreement between the equivalent reflections. In the case of the CTAC/*p*-PP complex, two phenyl rings were fixed to hexagon with C—C bonds restrained to 1.39 Å. Furthermore, all the bond lengths between carbon atoms were restrained to 1.52 Å with 0.005 weight, while atomic distances between C_{16} and C_{18}, and C_{17} and C_{19} were restrained to 2.55 Å with 0.020 weight to maintain appropriate values for bond angles of C_{16}—C_{17}—C_{18} and C_{17}—C_{18}—C_{19}, respectively. The final cycles of full-matrix least-squares refinement for CTAC/*p*-PP were based on 1,267 reflections, 283 parameters and 17 geometrical restraints.

The goodness of fit, final crystallographic R-(calculated based on F) and Rw-factors (calculated based on F^2, $w = 1/\sigma^2(Fo)$) were 1.66, 0.059, and 0.079 for CTAC and 1.27, 0.078 and 0.179 for CTAC/*p*-PP complex. The maximum and minimum peaks on the final difference Fourier map were 0.43 and −0.38 ($e/\text{Å}^3$) for CTAC and 0.14 and −0.13 ($e/\text{Å}^3$) for CTAC/*p*-PP. All calculations of data collection, structure determination and refinement were performed using a teXsan crystallographic software package of the Molecular Structure Corporation [10], SHELX-86 [9] and SHELX-93 [11], respectively. Final data may be obtained from the Cambridge Crystallographic Data Center, 12 Union Road, Cambridge, CB2 1EZ, UK.

RESULTS AND DISCUSSION

Phase Diagram of CTAC/*p*-PP System

Figure 1 shows TG and DTA curves of single crystals of the CTAC/*p*-PP complex with a 1/1 molar ratio crystallized from the solution. Single crystals obtained from the same batch were used for the X-ray data collection and

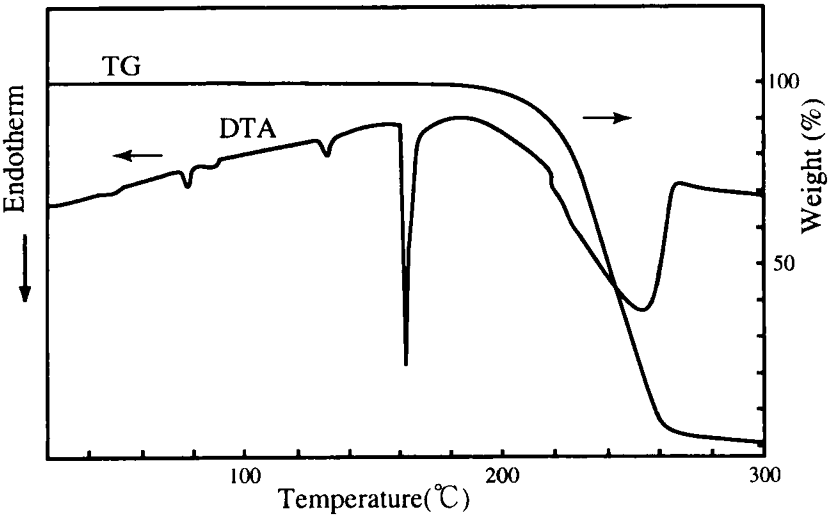

FIGURE 1 Thermogravimetric (TG) and differential thermal analysis (DTA) measurements for single crystals of the CTAC/*p*-PP complex with a composition of 1/1 molar ratio.

the thermal measurement. Essentially the same TG and DTA curves were obtained from the powder sample prepared by grinding CTAC and *p*-PP crystalline powder in a mortar with 1/1 molar ratio. The DTA curve consists of five endothermic peaks at 79, 87, 132, 163 and 254°C. Judging from the weight decrease starting from 200°C, the broad peak at 254°C can be assigned as its decomposition. The other four peaks seem to correspond to phase transition temperatures and these were plotted as data points at 1/1 molar ratio in the phase diagram (Fig. 2). The phase at room temperature (below 79°C) is a crystalline state according to the X-ray diffractions from the single crystal and equimolar mixture of CTAC and *p*-PP, in which many Bragg diffractions can be observed in the whole 2θ range. The phase above 163°C seemed to be a liquid-crystal state from an optical microscopic observation and an X-ray diffraction pattern, in which some Bragg diffractions and broad halo diffractions were observed. The details of other phases between the above transition temperatures were not investigated in

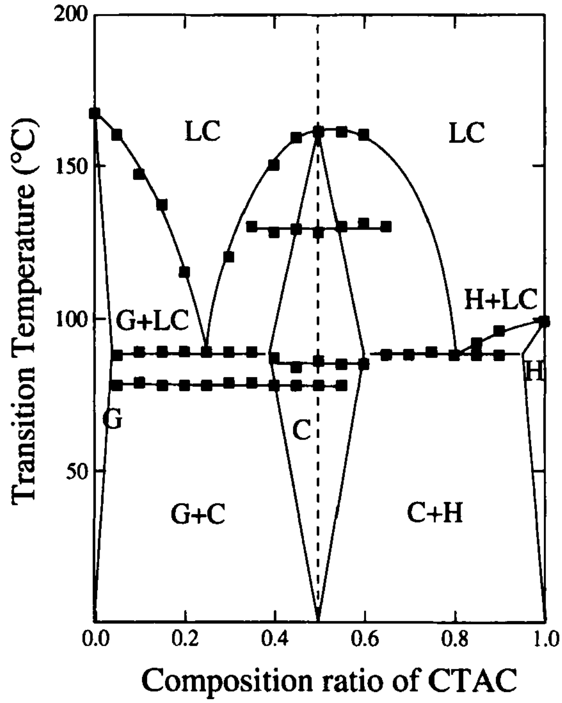

FIGURE 2 Temperature-composition phase diagram of the CTAC and *p*-PP system. Filled squares denote phase transition temperatures observed in DTA curves for each composition ratio.

this study. By changing the CTAC ratio from 0.0 to 1.0 at regular intervals, phase transition temperatures of mixed specimens were obtained from the DTA curve at every ratio. These were plotted as filled squares in Figure 2. Host (CTAC) and guest (*p*-PP) were mixed by grinding their powder samples in a mortar with a pestle to obtain individual composition ratios. From the data obtained, the phase boundary was estimated and shown as solid lines in the diagram. Although we didn't examine the details of each and every phase, phases of G, H, C, G + C, H + C, LC, G + LC and H + LC were confirmed by an X-ray diffraction method and an optical microscopic observation. Here, G, H, C and LC stand for the crystal state of guest, host, complex with 1:1 ratio, and liquid-crystal state, respectively. From this phase diagram, we may deduce the following conclusion. Since it has only one single peak at the composition ratio of 0.5 in this diagram, it is clear that only one complex with the host/guest ratio of 1/1 is possible for this system.

Molecular Structure of the CTAC and its Complex with *p*-PP

The molecular structure of the CTAC/*p*-PP complex with atomic numbering is shown in Figure 3. Similar atomic numbering was used in the case of the CTAC crystal. Since there are four CTAC molecules in an asymmetric unit of the CTAC crystal, the atomic numbering of the *j*-th atom in the *i*-th molecule is designated as N_i, Cl_i and C_{100i+j}. All the bond distances and angles of four CTAC molecules are in the normal range (Tab. II), from 1.493(6) to 1.524(6) Å for C—C and from 109.9(4) to 115.8(4)° for C—C—C, and from 1.481(6) to 1.517(5) Å for C—N and from 106.4(3) to 112.0(4)° for C—N—C. All the dihedral angles in the alkyl chain parts are in the range of 180±5°, with the exception of C_{204}—C_{205}—C_{206}—C_{207} (−172.7(4)°). These extended conformations of alkyl chains in the chloride salt are somewhat different from those in the bromide salts, where many dihedral angles deviate more than 10° from 180°, which causes the right- or left-handed twist of alkyl chains along the chain axis [12]. The alkyl chain in the CTAC/*p*-PP complex crystal has also an extended conformation (Tab. II, (c)), as found in many other complex crystals [6, 7, 8]. As shown in Figure 3, carbon atoms in the alkyl terminal region and in one of the phenyl rings ($C_{26} \sim C_{31}$) have larger temperature factors than those in the vicinity of ammonium cation and in the other phenyl ring ($C_{20} \sim C_{25}$), respectively. The reason for this will be discussed later.

Although two phenyl moieties of the *p*-PP molecule were constrained to the hexagon with the C—C bond length of 1.39 Å, the rotation of phenyl planes around C_{23}—C_{26} was freely allowed and the dihedral angle between

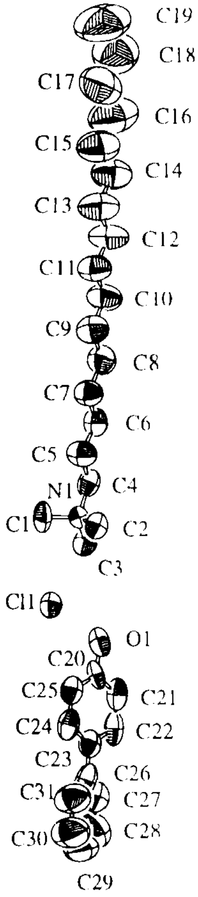

FIGURE 3 Molecular structures of CTAC and *p*-PP observed in the CTAC/*p*-PP complex crystal together with atomic numberings. Each atom is represented by the ellipsoids with 50% probability. Hydrogen atoms are not shown for the sake of clarity.

these two planes was found to be 28.2°. This value is close to one of the two common regions (around 0° and 30°) for the dihedral angle of biphenyl derivatives.

Packing Structures

The crystal structure of CTAC consists of smectic layers stacked along the *c*-axis (Fig. 4). In a smectic layer, alkyl chains linked to the nitrogen atoms at both sides of layer surfaces interdigitate mutually and make a hydrophobic

TABLE II Bond lengths, bond angles and dihedral angles of CTAC molecules in the CTAC and CTAC/*p*-PP crystals

(a) Bond lengths

	CTAC				CTAC/p-PP
	i=1	*i*=2	*i*=3	*i*=4	
N(i)—C(i01)	1.496(5)	1.499(6)	1.506(6)	1.491(6)	1.51(1)
N(i)—C(i02)	1.492(6)	1.510(6)	1.481(6)	1.494(6)	1.48(1)
N(i)—C(i03)	1.495(6)	1.496(5)	1.501(5)	1.506(6)	1.48(1)
N(i)—C(i04)	1.517(5)	1.514(5)	1.507(5)	1.517(5)	1.52(1)
C(i04)—C(i05)	1.498(6)	1.504(6)	1.493(6)	1.514(6)	1.514(5)*
C(i05)—C(i06)	1.511(6)	1.507(6)	1.524(6)	1.511(6)	1.520(5)*
C(i06)—C(i07)	1.508(6)	1.510(6)	1.516(6)	1.521(6)	1.515(5)*
C(i07)—C(i08)	1.519(6)	1.513(6)	1.511(6)	1.514(7)	1.510(5)*
C(i08)—C(i09)	1.518(6)	1.504(6)	1.515(6)	1.511(6)	1.520(5)*
C(i09)—C(i10)	1.503(7)	1.516(6)	1.509(6)	1.506(7)	1.514(5)*
C(i10)—C(i11)	1.517(6)	1.516(6)	1.514(6)	1.518(6)	1.517(5)*
C(i11)—C(i12)	1.505(7)	1.512(7)	1.502(6)	1.510(7)	1.517(5)*
C(i12)—C(i13)	1.518(6)	1.501(6)	1.508(6)	1.508(6)	1.516(5)*
C(i13)—C(i14)	1.510(6)	1.510(7)	1.503(7)	1.508(7)	1.517(5)*
C(i14)—C(i15)	1.512(6)	1.510(6)	1.511(6)	1.517(6)	1.519(5)*
C(i15)—C(i16)	1.512(6)	1.502(7)	1.510(7)	1.508(7)	1.516(6)*
C(i16)—C(i17)	1.516(6)	1.513(7)	1.508(6)	1.511(7)	1.520(6)*
C(i17)—C(i18)	1.503(7)	1.501(7)	1.507(7)	1.510(7)	1.524(6)*
C(i18)—C(i19)	1.508(7)	1.504(7)	1.509(8)	1.511(8)	1.513(6)*

*The bond length was restrained to 1.52 Å with 0.005 weight during refinement calculation by using the Shelx-93 program.

(b) Bond angles

	CTAC				CTAC/p-PP
	i=1	*i*=2	*i*=3	*i*=4	
C(i01)—N(i)—C(i02)	109.7(4)	109.6(3)	109.0(4)	108.5(4)	108.3(8)
C(i01)—N(i)—C(i03)	108.4(4)	108.3(3)	109.0(3)	109.3(3)	109.2(8)
C(i01)—N(i)—C(i04)	110.3(4)	107.5(3)	106.4(3)	112.0(4)	110.3(8)
C(i02)—N(i)—C(i03)	109.3(4)	108.6(3)	109.2(3)	108.2(3)	109.8(8)
C(i02)—N(i)—C(i04)	111.2(4)	111.2(3)	111.5(4)	107.7(3)	112.3(8)
C(i03)—N(i)—C(i04)	107.9(3)	111.6(3)	111.7(3)	111.0(3)	107.1(8)
N(i)—C(i04)—C(i05)	116.7(4)	115.4(4)	115.6(4)	114.9(4)	115.0(10)
C(i04)—C(i05)—C(i06)	109.9(4)	111.2(4)	111.9(4)	110.3(4)	112(1)
C(i05)—C(i06)—C(i07)	114.7(4)	113.6(4)	113.0(4)	112.9(4)	111(1)
C(i06)—C(i07)—C(i08)	113.2(4)	114.1(4)	115.7(4)	114.8(4)	113(1)
C(i07)—C(i08)—C(i09)	115.3(4)	114.3(4)	112.2(4)	113.9(4)	114(1)
C(i08)—C(i09)—C(i10)	113.9(4)	114.3(4)	115.6(4)	114.9(4)	115(1)
C(i09)—C(i10)—C(i11)	115.0(4)	114.5(4)	113.9(4)	114.5(4)	115(1)
C(i10)—C(i11)—C(i12)	114.4(4)	114.4(4)	115.8(4)	114.6(4)	111(1)
C(i11)—C(i12)—C(i13)	114.8(4)	114.5(4)	114.8(4)	114.6(4)	112(1)
C(i12)—C(i13)—C(i14)	114.9(4)	114.4(4)	115.4(4)	114.8(4)	115(2)
C(i13)—C(i14)—C(i15)	115.0(4)	115.0(4)	115.3(4)	115.1(4)	110(2)
C(i14)—C(i15)—C(i16)	114.3(4)	114.8(4)	114.9(4)	114.8(4)	103(2)
C(i15)—C(i16)—C(i17)	114.8(4)	115.4(4)	114.6(4)	114.9(4)	107(2)
C(i16)—C(i17)—C(i18)	114.8(4)	114.3(4)	114.9(4)	114.8(5)	110(1)**
C(i17)—C(i18)—C(i19)	114.2(5)	113.9(5)	114.5(5)	113.6(5)	112(1)**

**The bond angles were restrained by keeping distances of C(i16)···C(il8) and C(i17)···C(i19) to 2.55 Å with 0.02 weight during refinement calculation.

TABLE II (Continued)

(c) Dihedral angles

	CTAC				*CTAC/p-PP*
	i = 1	*i* = 2	*i* = 3	*i* = 4	
N(i)—C(i04)—C(i05)—C(i06)	117.1(4)	−173.7(4)	−178.3(4)	−178.1(4)	174(1)
C(i01)—N(i)—C(i04)—C(i05)	53.8(5)	−171.2(4)	−173.3(4)	67.4(5)	57(1)
C(i02)—N(i)—C(i04)—C(i05)	−68.2(5)	68.8(5)	67.9(5)	−173.4(4)	−64(1)
C(i03)—N(i)—C(i04)—C(i05)	172.0(4)	−52.6(5)	−54.6(5)	−55.1(5)	176(1)
C(i04)—C(i05)—C(i06)—C(i07)	175.2(4)	−172.7(4)	−176.4(4)	−177.1(4)	180(1)
C(i05)—C(i06)—C(i07)—C(i08)	−179.9(4)	179.9(4)	−178.7(4)	−179.8(4)	−180(1)
C(i06)—C(i07)—C(i08)—C(i09)	178.0(4)	−177.5(4)	−180.0(4)	−179.0(5)	176(1)
C(i07)—C(i08)—C(i09)—C(i10)	−179.1(4)	180.0(5)	179.6(4)	179.5(5)	−179(1)
C(i08)—C(i09)—C(i10)—C(i11)	179.1(4)	−179.7(5)	179.8(4)	−179.8(4)	179(1)
C(i09)—C(i10)—C(i11)—C(i12)	−179.2(5)	179.7(4)	180.0(4)	−180.0(4)	177(1)
C(i10)—C(i11)—C(i12)—C(i13)	179.9(4)	−179.5(4)	179.8(4)	−179.9(4)	179(1)
C(i11)—C(i12)—C(i13)—C(i14)	179.7(5)	−179.5(4)	−178.9(5)	−179.5(4)	−178(2)
C(i12)—C(i13)—C(i14)—C(i15)	179.8(4)	179.9(4)	179.8(4)	179.5(4)	177(2)
C(i13)—C(i14)—C(i15)—C(i16)	−179.0(4)	179.8(5)	−179.3(5)	−179.8(4)	179(2)
C(i14)—C(i15)—C(i16)—C(i17)	−179.9(4)	179.4(5)	179.4(5)	−179.3(4)	179(2)
C(i15)—C(i16)—C(i17)—C(i18)	−179.4(5)	179.4(5)	−179.7(5)	179.8(5)	178(2)
C(i16)—C(i17)—C(i18)—C(i19)	179.2(5)	−179.8(5)	179.7(5)	−179.8(5)	178(2)

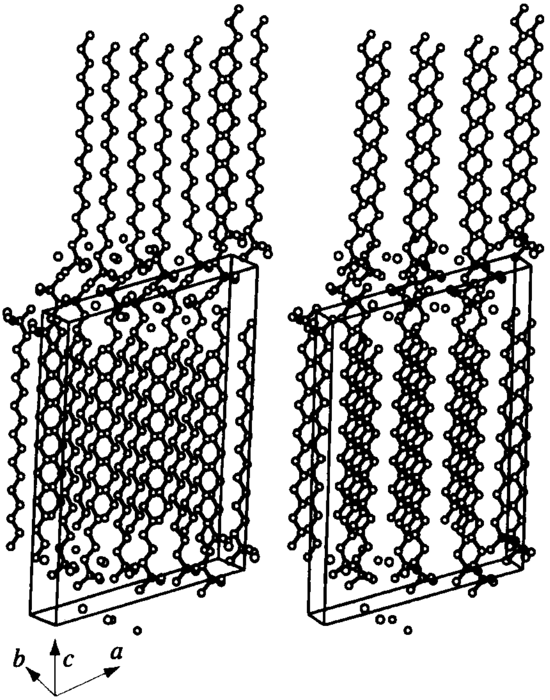

FIGURE 4 Stereo drawing of smectic layers of CTAC.

region. Since the mean deviation from the plane defined by 17 atoms of N_i, $C_{i04}, \ldots, C_{i19}$ in each chain is less than 0.077(5) Å, all four chains in an asymmetric unit have a good planarity. These four planes are almost parallel to each other with the largest angle of 5° between plane normals, and these are parallel to the crystallographic $(01\bar{1})$ plane. Except for two methylene moieties near the trimethylammonium cation, all the methylene moieties ($C_6 \sim C_{19}$) are sandwiched by those from the other side of the surface, which makes extra space in the hydrophilic region for chloride anions and water molecules. Ammonium cations and chloride anions are located at the layer surface, and they make a hydrophilic region together with two water molecules in an asymmetric unit. These two water molecules are linked to chloride anions by two hydrogen bonds, $Cl_1 \cdots O_1$ 3.238(4) and $Cl_3 \cdots O_1$ 3.258(4) Å with $Cl_1 \cdots O_1 \cdots Cl_3$ 118.0(1)°, and $Cl_1 \cdots O_2$ 3.236(4) and $Cl_2 \cdots O_2$ 3.214(4) Å with $Cl_1 \cdots O_2 \cdots Cl_2$ 113.2(1)° (Fig. 5). Although the Cl_4 anion does not participate in any hydrogen bond with water molecules, it has very short contact between one of the methyl carbon atoms, $Cl_4 \cdots C_{202}$ 3.267(5) Å. Taking into account that this methyl carbon atom links to the nitrogen cation, the observed short C_{202}—$H \cdots Cl_4^-$ interaction

FIGURE 5 Packing structure of the hydrophilic region of a CTAC crystal. Alkyl chains beyond C6 atom are excluded in this figure for the sake of clarity. Larger gray circles represent chloride anions and smaller circles represents water oxygen. Each CTAC molecule has a number from 1 to 4 to show the symmetrically equivalent molecule. Short atomic contacts are shown by dotted lines with contact length in Å.

can be reasonably described as a C—H···Cl hydrogen bond. Another plausible candidate for the C—H···Cl hydrogen bond was found between Cl_1 and C_{101} with 3.425(5) Å, which is slightly shorter than van der Waals distance, 3.45 Å, for these atoms. Other carbon atoms around chloride anions with a distance shorter than 3.65 Å are $Cl_1 \cdots C_{401}$ 3.564(5), $Cl_2 \cdots C_{102}$ 3.518(5), $Cl_3 \cdots C_{403}$ 3.515(5), $Cl_3 \cdots C_{302}$ 3.517(5), $Cl_3 \cdots C_{101}$ 3.639(5) and $Cl_4 \cdots C_{203}$ 3.554(5) Å. These observations clearly showed that the hydrophilic region of the CTAC crystal is packed very compactly. On the other hand, alkyl chains in the hydrophobic region are loosely packed in this crystal. For example, in this structure, there are seven short contacts between carbon atoms less than 3.90 Å. These are $C_{101} \cdots C_{301}$ 3.771(7), $C_{103} \cdots C_{303}$ 3.823(7), $C_{104} \cdots C_{218}$ 3.797(7), $C_{201} \cdots C_{203}$ 3.766(7), $C_{203} \cdots C_{302}$ 3.858(7), $C_{402} \cdots C_{403}$ 3.773(7), and $C_{403} \cdots C_{403}$ 3.88(1) Å. Only one interaction ($C_{104} \cdots C_{218}$ was found in the hydrophobic region. The rest of them were in the hydrophilic region.

In the CTAC/*p*-PP complex crystal, the interdigitation of alkyl chains from both sides of the layer surface becomes shallow and the smectic layer width elongates by about 5 Å. By loosening the interdigitation of alkyl chains, it became possible to accommodate a *p*-PP molecule in the space between the head and tail part of CTAC molecules (Fig. 6). The resulting complex compound has the 1:1 molar ratio of CTAC/*p*-PP. Here, for convenience, we shall call CTAC a host, and *p*-PP a guest molecule. The guest *p*-PP molecule links to the chloride anion by a strong hydrogen bond with a Cl···O distance of 3.011(8) Å and a Cl···H—O angle of 172° (Fig. 7). There is another noticeable short contact between O and one (C_1) of the methyl carbon atoms linked to the ammonium nitrogen with a distance of 3.13(1) Å. For the same reason as mentioned for the short contact between Cl_4 and C_{202} in CTAC crystal, this is described as C—H···O hydrogen bond. Because of these hydrogen bonds between hydroxyl moieties of *p*-PP, Cl^- and methyl moieties in the hydrophilic region together with electrostatic interactions between N^+ and Cl^- (3.97 and 3.99 Å), the thermal movement of atoms in this region is restricted to a certain extent as compared with that in the hydrophobic region. This was clearly shown in Figure 3, in which the size of the atom corresponded to the magnitude of its temperature factor.

The most interesting structural feature found in this complex crystal is the arrangement of host and guest molecules. In many complex crystals [5, 7, 8] including the dodecyltrimethylammoniumbromide (DTAB)/*p*-PP complex [6], guest aromatic molecules were packed isolately within a space obtained by loosening the mutual interdigitation of alkyl chains, so that there is no specific interaction between guest molecules. Guest molecules in the CTAC/

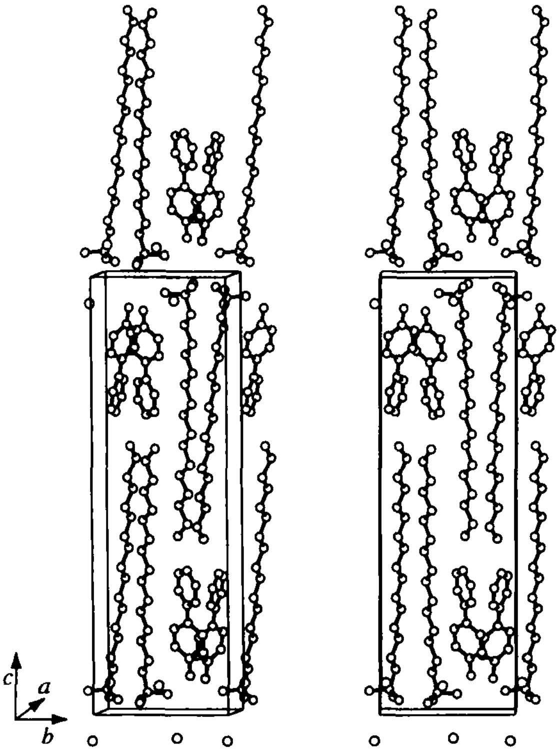

FIGURE 6 Stereo drawing of smectic layers of CTAC/*p*-PP.

p-PP complex, however, seem to have some guest–guest interactions since the herring-bone structure of guest molecules was found in the complex crystal, which is very similar to that found in the guest single crystals [14]. Host molecules also show the herring-bone structure because of a glide symmetry along the *a*-axis. Although the planarity of the alkyl chain is very good (the mean deviation from the plane defined by 17 atoms from N to C_{19} is 0.085 Å) as in the CTAC crystal, the neighboring alkyl planes are almost perpendicular (about 70°), which is very different from the parallel packing in the CTAC crystal.

The crystal-liquid crystal transition temperature (163°C) and its peak profile of the CTAC/*p*-PP complex crystal (Fig. 1) is very similar to the melting temperature (168°C) and its peak profile of guest crystals. These structural and thermal similarities between the CTAC/*p*-PP complex and the *p*-PP crystal suggest that the complex crystal structure is influenced largely by the guest *p*-PP packing structure. Therefore, we may call this type of

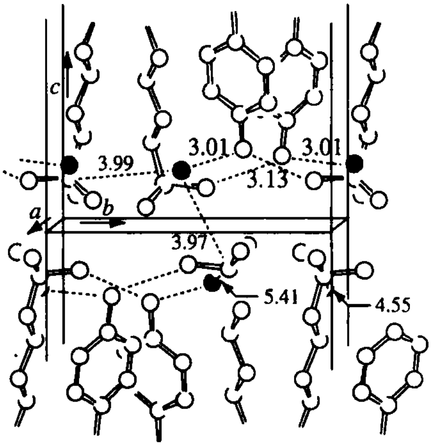

FIGURE 7 Packing structure of the hydrophilic region of the CTAC/*p*-PP complex. Gray circles represent chloride anions. Some short atomic contacts are shown by dotted lines with contact length in Å.

structure a "guest-dependent" packing structure. The other complexes belonging to this packing structure and observed so far were the dodecyltrimethylammonium chloride (DTAC)/*p*-PP and the DTAC/*p*-iodophenol complex [13]. On the other hand, most of the other complexes obtained so far have a "host-dependent" packing structure, where the packing structure of complex crystals is very similar to that of host crystals and no specific interaction between guest molecules is found.

References

[1] K. Okuyama, Y. Soboi, N. Iijima, K. Hirabayashi, T. Kunitake and T. Kajiyama, *Bull. Chem. Soc. Jpn.*, **61**, 1485 (1988).
[2] K. Okuyama, N. Iijima, K. Hirabayashi, T. Kunitake and M. Kusunoki, *Bull. Chem. Soc. Jpn.*, **61**, 2337 (1988).
[3] A. R. Campanelli and L. Scaramuzza, *Acta Crystallogr.*, **C42**, 1380 (1980).
[4] H. Hirata and Y. Sakaiguchi, *Bull. Chem. Soc. Jpn.*, **62**, 581 (1989).
[5] K. Vongbupnimit, K. Noguchi and K. Okuyama, *Mol. Cryst. Liq. Cryst.*, in press.
[6] S. Kamitori, Y. Sumimoto, K. Vongbupnimit, K. Noguchi and K. Okuyama, *Mol. Cryst. Liq. Cryst.*, in press.
[7] F. Toda, K. Tanaka, T. Okada, S. A. Bourns and L. R. Nassimbeni, *Supramol. Chem.*, **3**, 291 (1994).
[8] K. Noguchi, K. Okuyama and K. Vongbupnimit, *Mol. Cryst. Liq. Cryst.*, **276**, 185 (1996).
[9] G. M. Sheldrick, *Crystallographic Computing*, **3**, Oxford University Press, 175–188 (1985).
[10] TeXsan, Crystal Structure Analysis Package, Version 1.6, Molecular Structure Corporation, The Woodlands, TX 77381 (1993).
[11] G. M. Sheldrick, SHELXL93, Program for Crystal Structure Refinement, Univ. of Goettingen, Germany (1993).

[12] Y. Nakadai, K. Noguchi and K. Okuyama, in preparation.
[13] K. Vongbupnimit, K. Noguchi and K. Okuyama, in preparation.
[14] C. P. Brock and K. L. Haller, *J. Phys. Chem.*, **88**, 1370 (1984).